

Low-profile Normal-Mode Helical Antenna for Use in Proximity to Metal

Wongook Hong, Naobumi Michishita and Yoshihide Yamada

Department of Electrical and Electronic Engineering
National Defense Academy
1-10-20 Hashirimizu, Yokosuka-shi, 239-8686 JAPAN
yyamada@nda.ac.jp

Abstract— To expand the applicability of UHF tags, a low-profile, small, normal-mode helical antenna (NMHA) that can be used on metallic plates was developed. This paper clarifies the design method for antenna structures for use in proximity to metal. The design data were obtained with the electromagnetic simulator FEKO. Fundamental electrical characteristics such as the antenna input impedances, self-resonance conditions, and radiation characteristics were clarified in proximity to metal. For antenna sizes of $0.03\text{--}0.05$ wavelengths, antenna gains of about -0.5 dBd were achieved. The calculated results were verified using an actual antenna (size, 0.04 wavelengths). A tap feed structure was used for impedance matching. It was shown that very precise design results could be achieved. Moreover, the developed NMHA was designed to be a tag antenna. Here, the antenna impedance was matched to the IC chip impedance. The read range of the developed tag was measured to be about 15 m.

Index Terms— Tag antenna, Normal Mmode Helical Antenna, Metal Proximity Use and Read Range.

I. INTRODUCTION

Radio-frequency identification (RFID) systems have recently attracted much interest for use in efficiently tracking and identifying objects in various supply chains [1]. An RFID system basically consists of a reader, writer, and tag. For UHF tags, film-type half-wavelength (0.5λ) dipole antennas are used as antennas in many applications [2]. However, such tag antennas cannot be mounted on metallic objects or bottles full of liquids because the antenna characteristics are seriously degraded by the resulting change in antenna impedance [3]. For

these applications, some designs for patch antennas [4] and slot antennas [5] were proposed. Nevertheless, although these antennas were sufficiently thin—some less than 4 mm—they were about 80 mm in size, which limited them to specialized applications. This limitation was overcome in the design of a small, normal-mode helical antenna (NMHA) that could be used on metallic plates [6]. An antenna gain of -0.4 dBd was achieved by an antenna that was 0.035λ (11 mm) in size in proximity to metal. However, the antenna thickness was as large as 9 mm. This must be reduced to increase user convenience.

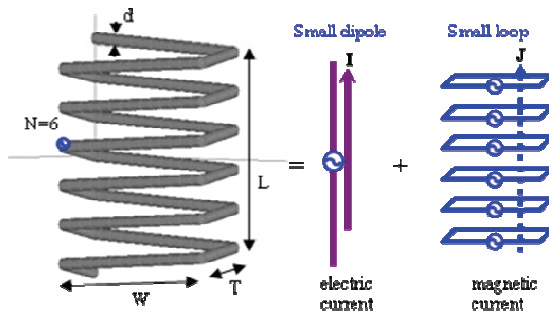
In this study, projection was reduced by using a rectangular cross section for the NMHA. This rectangular NMHA was designed using the commercial electromagnetic simulator FEKO Suite 5.4 [7]. The simulation parameters were verified to ensure precise calculations, and the fundamental electrical performance characteristics such as the antenna input impedances, self-resonance condition, and radiation characteristics were calculated in proximity to metal. For antenna sizes of $0.03\text{--}0.05\lambda$, antenna gains of about -0.5 dBd were achieved. The calculated results were confirmed using an actual antenna with the size 0.04λ . A tap feed structure was designed for impedance matching. It was shown that very precise design results could be achieved. Moreover, the developed NMHA was designed to be a tag antenna. Here, the antenna impedance was matched to the IC chip impedance. The read range of the developed tag was measured to be about 15 m.

II. FEATURES OF THE RECTANGULAR NMHA

The configuration of the rectangular NMHA is

shown in Fig. 1(a). L and W represent the antenna length and width, respectively. The number of turns in the helix is represented by N . The antenna wire has the diameter d . The NMHA has a rectangular cross section. The projection from the metal is expressed by T . This projection was decreased sufficiently.

Electrically, the proposed NMHA is equivalent to the small dipole and loops shown in Fig. 1(b). And because the capacitance of the small dipole is cancelled out by the inductance of the loops—a condition called self-resonance—a purely resistive input impedance can be achieved. This is very important for effective radiation. When this antenna is placed near a metal plate, although the performance of the small dipole is degraded, the performance of the loop antenna is enhanced. Therefore, this antenna works well even in proximity to metal.



(a) Perspective view (b) Electrical equivalent configuration

Fig. 1. Configuration of the rectangular NMHA.

III. SIMULATION CONDITIONS

In order to calculate precisely, the simulation parameters were studied. The commercial electromagnetic simulator FEKO was employed. A simulation example is shown in Fig. 2. The antenna was placed on a metal plate with a 1 mm spacing. The most important parameter to obtain for exact results was the segment size (ΔS) of the metal plate near the antenna, as shown by the red frame. Table 1 gives the simulation parameters. Because the antenna length was very small, such as about $\lambda/25$, the antenna segment size was set at $\lambda/500$. As for the metal plate mesh sizes, $\lambda/20$ was used outside the red frame. Inside the red frame, the mesh sizes were varied from $\lambda/10$ to $\lambda/80$ so as to check the convergence of the calculated results. Other calculation data for the

memory size and calculation time showed that the computational load was very light.

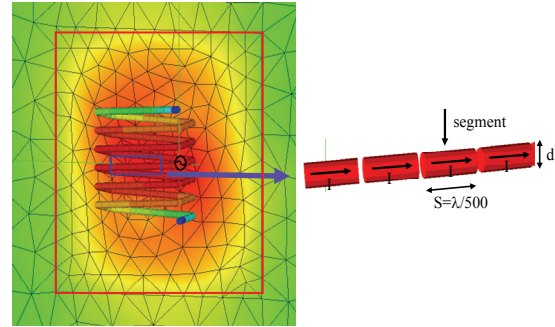


Fig. 2. Current distributions of NMHA structure.

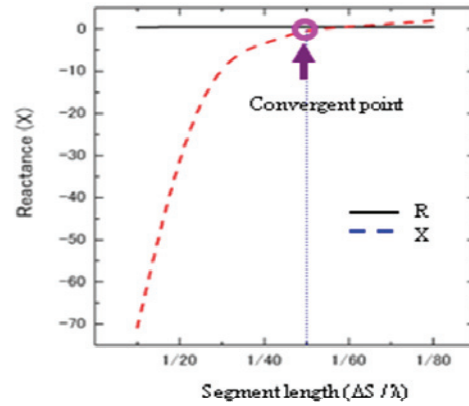


Fig. 3. Convergence of the input impedance.

Table 1: Simulation parameters.

Computer	CPU	2.8 GHz
	Memory	7.9 GByte
Simulator	MOM of FEKO	
Frequency	953 MHz	
Segment size	Antenna	$\lambda/500$
	Metal plate (near the ant.)	$\lambda/10$ to $\lambda/80$
	Metal plate (far from the ant.)	$\lambda/20$
Number of segments	Antenna	348
	Metal plate	5,448
Calculation memory size	Antenna	696 KByte
	Metal plate	120 MByte
Calculation time (seconds)	Antenna	0.94
	Metal plate	139

Fig. 3 shows the convergence of the input impedance calculations. This antenna was designed to satisfy the self-resonant condition. Consequently, the reactance of the input impedance should become zero. At a segment size of $\lambda/50$, the reactance approached zero. Hence, a mesh size of $\lambda/50$ was used in the red frame area. The input resistance was not affected by the segment size.

IV. CALCULATED DESIGN DATA

The simulation configuration is shown in Fig. 4. The antenna thickness is expressed by T . The size of the metal plate is expressed by M . The spacing between the antenna and the metal plate is expressed by S . The equivalent electric and magnetic currents are indicated by I and J , respectively. As for the radiation components, E_θ and E_ϕ correspond to the radiation from the electric and magnetic currents, respectively.

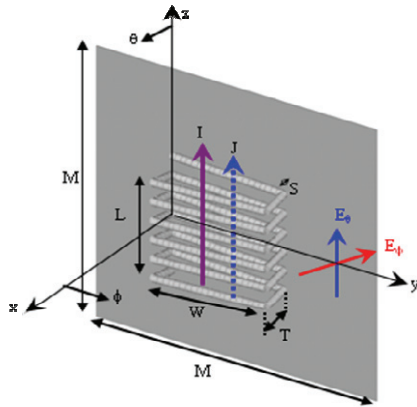


Fig. 4. Simulation configuration.

In the antenna configuration design, the most important design subject is the self-resonance condition. In the self-resonance condition, the capacitance and inductance of the input impedance are cancelled out. The antenna length L determines the input capacitance ($-X_D$) of the short dipole. The cross-sectional area of the antenna, given by the antenna width W and the thickness T , determines the input inductance (X_L). The total input inductance can be found by multiplying by the number of turns N . So, for a given L , combinations of W , T , and N were determined. The relations of these parameters are shown in Fig. 5. In this case, T and N are given as variable parameters. Other parameters,

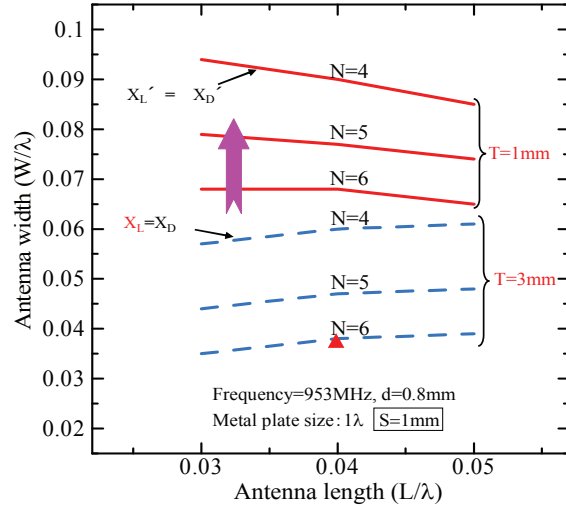


Fig. 5. Self-resonance for various T .

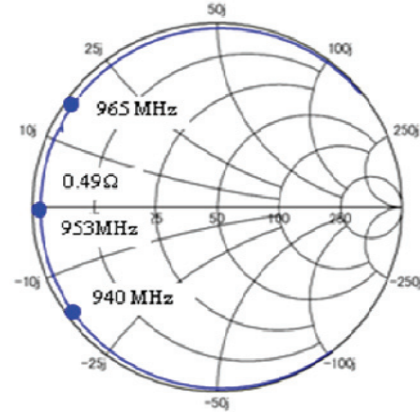


Fig. 6. Input impedances.

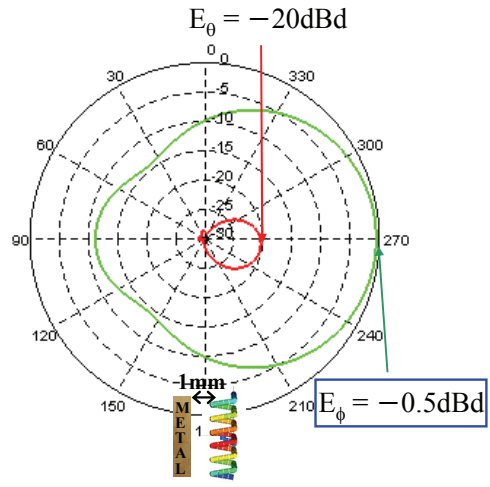


Fig. 7. Radiation patterns.

such as the wire diameter (d), spacing (S), and metal size (M) are shown in the figure. For smaller values of T , larger W values were needed in order to maintain the cross-sectional area. For

smaller values of N , larger W values were needed in order to increase the individual inductances of the cross-sectional areas. It is remarkable that all of the curves were almost unaffected by a change in L .

An example of the input impedance at the structure indicated by the triangular mark at $T = 3$ mm is shown in Fig. 6. At 953 MHz, the input impedance became a pure resistance of 0.49Ω . Because the antenna had a very small length of 0.04λ , the input resistance became very small. The radiation characteristics are shown in Fig. 7. In order to estimate the radiation level conveniently, the input impedance mismatch was ignored by utilizing a “no mismatch” calculation condition. The dominant radiation component became E_ϕ , which corresponded to

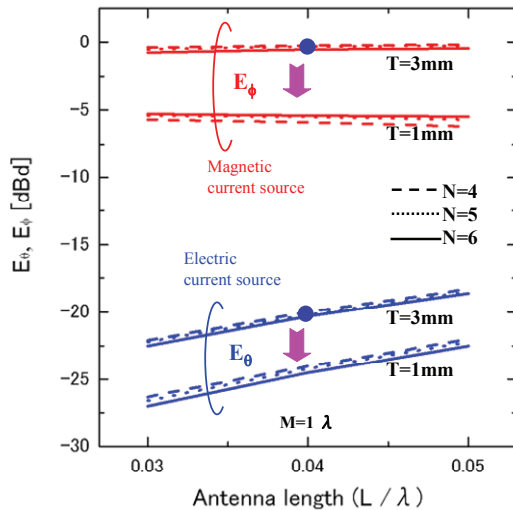


Fig. 8. Gain for various T .

the magnetic current source. It was surprising that an antenna gain of -0.5 dBd was obtained, which was comparable to a 0.5λ dipole antenna. Here, the unit dBd represents the antenna gain normalized by that of the 0.5λ dipole antenna. The high gain is due to the adequate ohmic resistance (R_o) in relation to the radiation resistance (R_r). R_o is determined by the antenna wire length and diameter (d). Here, because R_r is 0.24Ω , R_o should be smaller than R_r . To achieve a very small resistance, the wire diameter should be as large as possible. For $d = 0.8$ mm, $R_o = 0.25 \Omega$. Then, the antenna radiation efficiency is about 50%. This confirms the practicality of this small rectangular NMHA when used in proximity to metal.

The important antenna gain characteristics under the self-resonance condition are shown in Fig. 8. It is remarkable that the E_ϕ components were dominant. The E_θ components became less than -20 dBd. As for N changes, no antenna gain differences were observed. For larger T values, high gains were achieved. For $T = 3$ mm, antenna gains comparable to that of a 0.5λ dipole antenna are expected. One more feature was that the antenna gains remained constant for different L . Hence, it is expected that excellent antenna gains are probable for very small antenna sizes such as 0.03λ .

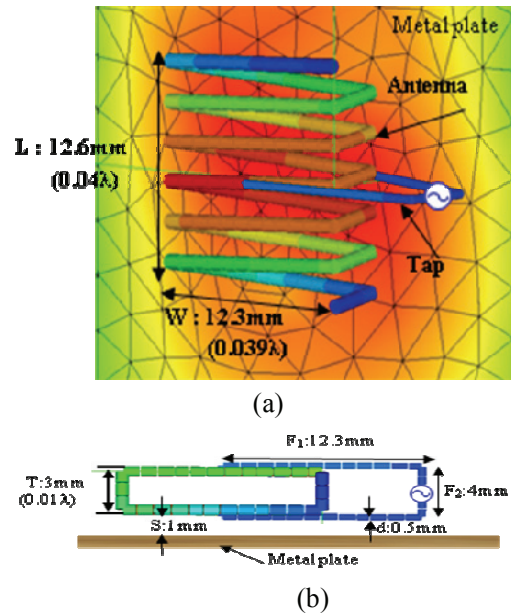


Fig. 9. (a) Perspective view and (b) cross-sectional view of the experimental NMHA structure.

V. PRACTICAL ANTENNA DESIGN

The previous section showed that high antenna gains can be expected in the very small NMHA. However, because the input resistance is very small, an antenna impedance matching structure is needed for practical application. This section shows how such a matching structure can be achieved. A tap type matching structure [8] was employed, as shown in Fig. 9(a) and (b). The tap was composed of a single U shaped wire. One end of the wire was connected to the antenna conductor. A feed point was placed at the other end. Wire diameters of 0.8 mm and 0.5 mm were selected for the antenna and the tap, respectively. Fig. 9(b) shows that the tap arms were placed

between the antenna wires in order to avoid increasing the antenna thickness [9]. Because the spacing between the antenna and the metal plate was very small (1 mm), the arrangement of the tap arms was very important.

The actual parameters are shown in Fig. 9. In order to verify the electrical performance characteristics of the antenna through measurements, the antenna input impedance was matched to the coaxial cable impedance of 50 Ω. The tap structure of this case is considered to be rather simple.

The fabricated antenna and feed cable are shown in Fig. 10. The tap arms were soldered to the antenna wire. A coaxial cable was used as a feed line. A sperrtopf balun was attached to the coaxial cable to suppress the leak currents on the coaxial cable. Fig. 11 shows the measured and calculated antenna impedances. The measured and calculated results agreed very well with and without tap feeds. When the tap feed was employed, the antenna impedance became exactly 50 Ω. The effectiveness of the tap feed was thus verified. The bandwidth characteristics are shown in Fig. 12. A 3.5 MHz bandwidth was obtained when VSWR < 2. This bandwidth corresponded to 0.4% of the center frequency.

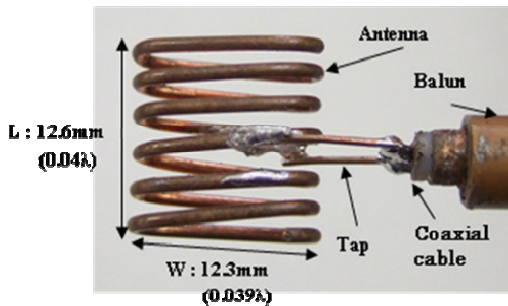


Fig. 10. Photograph of the fabricated antenna.

The radiation characteristics were verified through measurements. Fig. 13 shows the data for the case without the metal plate. The measured and calculated results agreed very well. Therefore, the achievement of the designed results was verified. In this case, the E_θ component corresponding to the electric current source became dominant. An antenna gain of about -2.9 dBd was achieved. By taking into account the small antenna size of 0.04λ , this antenna gain seems surprisingly large. However, the E_ϕ component, which corresponded to the magnetic current source, became small, such as -11 dBd.

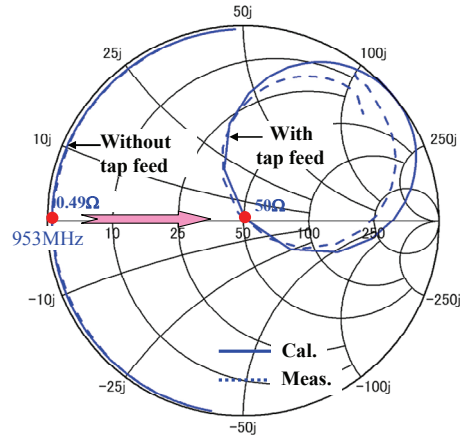


Fig. 11. Input impedances with and without tap feed.

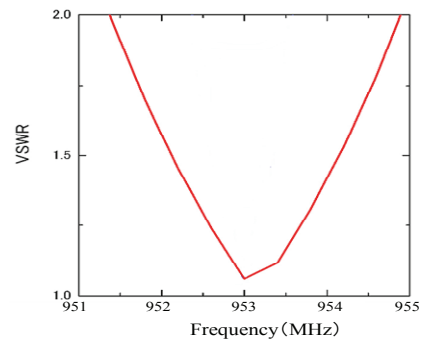


Fig. 12. The characteristics of the VSWR.

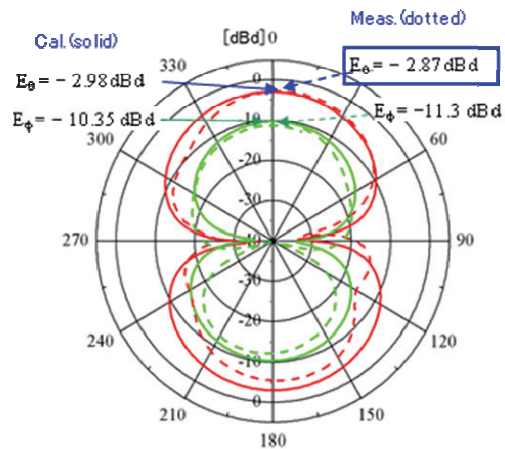


Fig. 13. Radiation patterns without metal plate.

The important radiation characteristics with a metal plate are shown in Fig. 14. In this case, the antenna was placed on the metal plate with $S = 1$ mm. A square metal plate with a size of 0.5λ was employed. The E_ϕ component became dominant in the case of metal proximity. A very

high antenna gain of -0.5 dBd was achieved. The E_ϕ level was increased by about 10 dB compared to the case without the metal plate. The usefulness of the NMHA in a metal proximity application was verified. At the same time, the intensity of the E_θ component decreased to -11 dBd. This showed that the electrical current source no longer worked well in proximity to the metal.

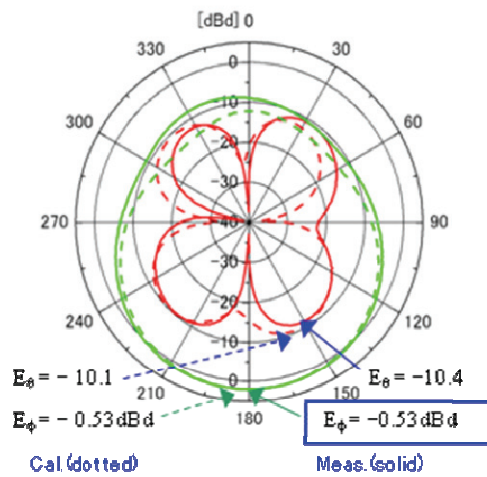


Fig. 14. Radiation patterns with metal plate.

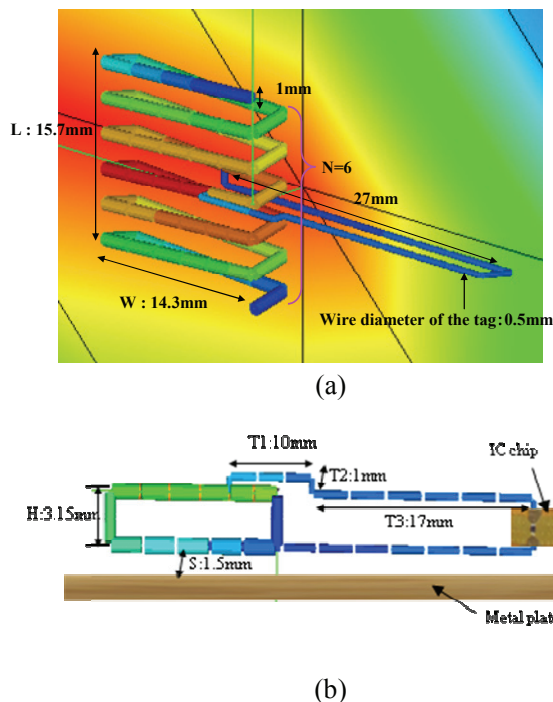


Fig. 15. (a) Perspective view and (b) cross-sectional view of the antenna structure matching IC chip.

VI. TAG ANTENNA DESIGN

In order to use the rectangular NMHA as a tag antenna, the antenna input impedance had to be matched to the IC chip impedance of $Z_{IC} = 25 - j95 \Omega$. Therefore, the antenna size and tap size were modified as shown in Fig. 15. The tap length was elongated in order to produce the inductance that was needed to achieve conjugate matching to the IC chip capacitance. The spacing between the antenna and the metal plate was set to 1.5 mm. As for the metal plate, a 0.5λ square plate was employed.

The impedance matching process is shown in Fig. 16. It was recognized that the tap length (T_3) was very important in the matching to the IC chip. Almost complete conjugate matching could be achieved at $T_3 = 17$ mm.

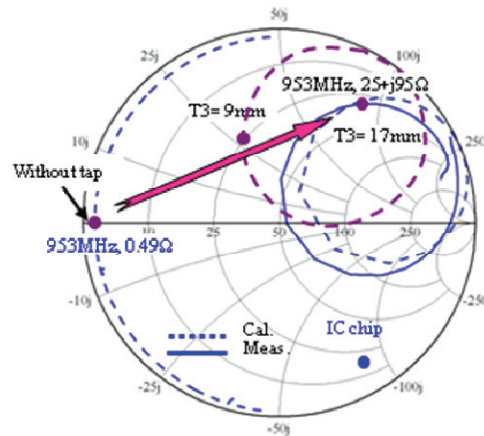


Fig. 16. Input impedances.

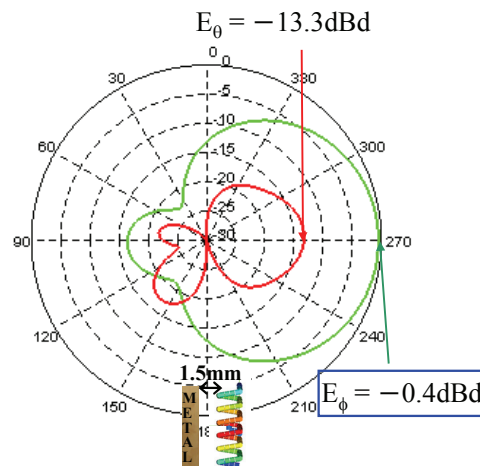
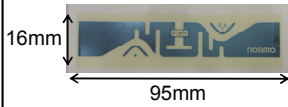
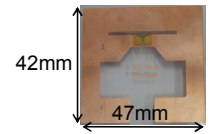
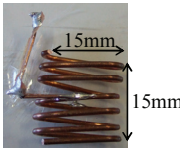
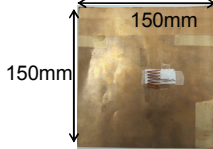


Fig. 17. Estimated radiation patterns.

Table 2: Measured read ranges.

	Antenna alone	Read range	Antenna alone	Read range
Current Antenna		9m		9m
Low profile NMHA	Antenna alone	Read range	Metal plate (150mm × 150mm)	Read range
		6m		15m

In order to estimate the antenna gain of this structure, the radiation characteristics were calculated, and the results are shown in Fig. 17. In this case, the antenna input impedance was designed to be $Z_{ANT} = 25 + j95 \Omega$. In order to easily calculate the radiation intensity, the input impedance mismatch was ignored by utilizing the “no mismatch” calculation condition. An antenna gain of -0.4 dBd was obtained. Therefore, an electrical performance comparable to conventional tags can be expected.

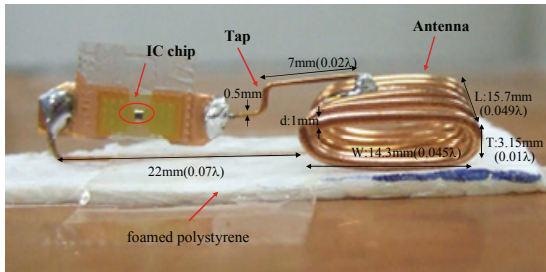


Fig. 18. The RFID tag structure using the NMHA.

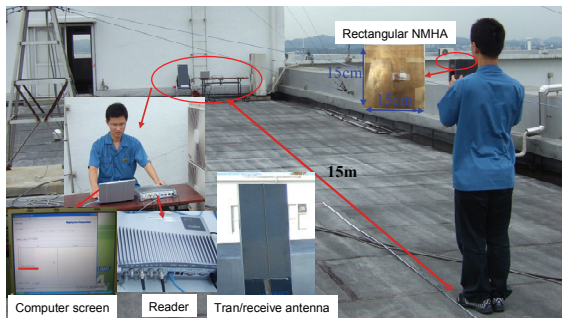


Fig. 19. Read range measurement.

VII. READ RANGE

The final estimation of the electrical performance of a tag is the read range. The tag configuration of the rectangular NMHA is shown in Fig. 18. The IC chip was inserted in the tap arm. The antenna and IC chip were placed on a piece of polystyrene foam attached to the metal plate. The thickness of the foam was 1.5 mm. The size of the metal plate was 0.5λ square. The read range was measured with the setup shown in Fig. 19. A commercial reader antenna was used for transmitting and receiving. This reader antenna was connected to a reader unit and a computer. When the tag information was read, the tag number was indicated on the computer screen.

Read range measurement were conducted by changing the distance between the reader antenna and the tag. The distance where the tag number disappeared was considered the read range. These read ranges might be affected by the height pattern at the measurement site. So, in every case, the height of the tag was selected so as to obtain the highest electrical strength.

The measured read ranges of some types of tags are summarized in Table 2. In the case of conventional antennas, read ranges of 9 m are obtained. In the case of the NMHA, read ranges of 6 m and 15 m were obtained without and with metal plate proximity, respectively. The effectiveness of the developed tag was verified through this read range measurement

VIII. CONCLUSIONS

A low profile, small NMHA was developed

for use on the surface of a metal plate. Important design data were obtained through simulations using the electromagnetic simulator FEKO. The following novel technical results were obtained.

- (1) The structural conditions for $0.03\text{--}0.05\lambda$ antennas were obtained.
- (2) The antenna gain design data for metal proximity applications were obtained. A nearly -0.5 dBd gain was shown.
- (3) In order to fabricate a practical antenna, a tap type matching structure was designed to match the antenna impedance to a $50\ \Omega$ cable or IC chip impedance.
- (4) The read range characteristics of the NMHA tag were obtained through measurements. A read range of about 15 m was verified.

ACKNOWLEDGMENT

The authors would like to thank the president, K. Kabumoto, and the executive director, T. Hiarano, of Mighty Card Co-op. for their continuous support of this study.

REFERENCES

- [1] RFID-related presentations, Special sessions at *IEEE AP-S International Symposium*, Honolulu, HI, June 2007.
- [2] H.W. Son, G. Y. Choi, and C. S. Pyo, "Open-Ended Two Strip Meander-Line Antenna for RFID Tags," *ETRI Journal*, vol. 28, no. 3, pp. 383-385, June 2006.
- [3] L. Ukkonen, M. Schaffrath, L. Sydanheimo and M. Kivikoski, "Analysis of integrated slot-type tag antenna for passive UHF RFID," *IEEE AP-S International Symposium*, pp. 1343-1346, July 2006.
- [4] M. L. Ng, et al, "Design and Miniaturization of an RFID Tag Using a Simple Rectangular Patch Antenna for Metallic Object Identification," *IEEE AP-S International Symposium*, pp. 1741-1744, June 2007.
- [5] X. Zeng, et al, "Slots in Metallic Label as RFID Tag Antenna," *IEEE AP-S International Symposium*, pp. 1749-1752, June 2007.
- [6] W. G. Hong, W. H. Jung, Y. Yamada and N. Michishita, "High Performance Normal Mode Helical Antenna for RFID Tags," *IEEE AP-S International Symposium*, pp. 6023-6026, June 2007.
- [7] www.feko.info
- [8] C. A. Balanis, "Antenna Theory Analysis and Design, Second Edition", John Wiley & Sons Inc., Ch. 9, pp. 472-480, 1997.
- [9] W. G. Hong, Y. Yamada and N. Michishita, "Design of a simple tap structure for low profile small normal mode helical antenna," *IEEE AP-S International Symposium*, no. 229, vol. 5, July 2008.



Won Gook Hong was born in Pusan, Korea on June 23, 1976. He enlisted in the Republic of Korea Army in 1999. He began as a platoon leader. Now he is a Captain. He entered the master course for

Electronics Engineering at the National Defense Academy, Kanagawa, in 2007. His current research interests include tag antennas and reader antennas for RFID.



Naobumi Michishita received the B.E., M.E., and D.E. degrees in Electrical and Computer Engineering from Yokohama National University in 1999, 2001, and 2004, respectively. He

joined the Department of Electrical and Electronic Engineering, National Defense Academy, as a research associate in 2004. He was a visiting scholar at the University of California, Los Angeles from 2006 to 2007. He received the Young Engineer Award from the IEEE AP-S Japan Chapter and IEICE in 2004 and 2005, respectively. His current research interests include metamaterial antennas and electromagnetic analysis. He is a member of IEEE.

**Yoshihide Yamada**

graduated from the Nagoya Institute of Technology and received the BS and MS degrees in electronics in 1971 and 1973, respectively. He received the DE degree from the Tokyo Institute of Technology in 1989. In 1973, he joined the Electrical Communication Laboratories of the Nippon Telegraph and Telephone Corporation (NTT). Until 1984, he was engaged in research and development related to reflector antennas for terrestrial and satellite communications. Beginning in 1985, he engaged in R&D for base station antennas for mobile radio systems. In 1993, he moved to the NTT Mobile Communications Network Inc. (NTT DoCoMo). In 1995, he was temporarily transferred to the YRP Mobile Telecommunications Key Technology Research Laboratories Co., Ltd. At the same time, he was a guest professor at the cooperative research center of Niigata University, and a lecturer at the Science University of Tokyo, both from 1996. In 1998, he took a position as a professor at the National Defense Academy. At present, he is interested in very small RFID antennas, shaped dielectric lens antennas, and electromagnetic simulations of large objects.

He is a member of the IEICE and JSST of Japan and an IEEE society member of AP, VT, and COMM.